Topographic Heterogeneity in Transdermal Transport Revealed by High-Speed Two-Photon Microscopy: Determination of Representative Skin Sample Sizes

Betty Yu, Ki Hean Kim,* Peter T. C. So,* Daniel Blankschtein, and Robert Langer

Department of Chemical Engineering and *Department of Mechanical Engineering, Massachusetts Institute of Technology, Cambridge, Massachusetts, U.S.A.

A novel application of high-speed two-photon microscopy was utilized to determine the optimum number of skin sites required to accurately determine the changes in transdermal transport properties incurred globally, over a clinically relevant area of skin. In contrast to the four to six skin sites (100 μm by 100 μm area per site) examined previously, this study accounted for the fluorescent probe distributions at 400 consecutive skin sites, covering a total skin area of 2 mm by 2 mm. The oleic-acid-induced changes in the transdermal transport properties of the model hydrophobic probe, rhodamine B hexyl ester, and of the model hydrophilic probe, sulforhodamine B, for this 400-skin-site study exhibited different dependencies on sample size for each probe. Whereas the examination of six skin sites captures the relative changes in the global transdermal transport properties of the hydrophobic probe, the valid assessment of these changes for the hydrophilic probe requires a significantly larger sample size of at least 24 skin sites. ***Key words: chemical enhancement mechanism/excised human cadaver skin/fluorescent probe/high-speed two-photon microscopy/oleic acid/skin sample size. J Invest Dermatol 118:1085–1088, 2002***

The recent application of two-photon microscopy (TPM) to visualize model drug spatial distributions across human cadaver skin has enabled the noninvasive elucidation of oleic-acid-induced changes in transdermal transport properties (Yu *et al*, 2001). Compared with other visualization techniques, the advantages of TPM include increased three-dimensional depth discrimination, increased signal collection efficiency, and reduced skin sample photobleaching and photodamage (Masters *et al*, 1997). In these previous studies, the quantification of the relative changes (enhancement values) in the vehicle to skin partition coefficient E_K, the skin intensity gradient E_g, the skin diffusion coefficient E_D, and the skin barrier thickness E_l of the probes used was based on a limited sampling of four to six different skin sites per skin sample, where each skin site covers 100 μm by 100 μm. Moreover, the site to site variations in probe spatial distributions were attributed to the intrinsic heterogeneity of the skin morphology (Yu *et al*, 2001). Although the morphologic variations in skin topology have been pertinent to dermatologic research (Huzaira *et al*, 2001), the consequences of skin morphology on the variability of transdermal permeant distributions over a clinically relevant skin area have not yet been addressed.

Manuscript received September 28, 2001; revised February 2, 2002; accepted for publication February 19, 2002.

Reprint requests to: Dr. Daniel Blankschtein, Department of Chemical Engineering, Room 66-444, Massachusetts Institute of Technology, 77 Massachusetts Avenue, Cambridge, MA 02139-4307; Email: dblank@mit.edu; or Robert Langer, Department of Chemical Engineering, Room E25-342, Massachusetts Institute of Technology, 77 Massachusetts Avenue, Cambridge, MA 02139-4307; Email: rlanger@mit.edu

Abbreviations: HTPM, high-speed two-photon microscopy; RBHE, rhodamine B hexyl ester; SRB, sulforhodamine B; TPM, two-photon microscopy.

In this study, the permeant spatial distributions over 400 consecutive sites in excised human cadaver skin were captured to reveal the variability of transdermal transport over a more clinically relevant area of 2 mm by 2 mm, using high-speed two-photon microscopy (HTPM) (Kim *et al*, 1999). The restriction to small sample sizes (four to six skin sites) in the earlier study (Yu *et al*, 2001) was largely due, to the slow image acquisition times (0.5 h per skin site), which are typical of instruments with microscopic resolution such as conventional TPM imaging systems. The development of HTPM has subsequently increased data acquisition rates by two orders of magnitude (Kim *et al*, 1999), thus enabling the scanning of multiple skin sites per sample over a relatively short period of time. Specifically, for the 400 skin sites examined here, the total scanning time remains below 1.5 h, compared with the 200 h required by the conventional TPM for the same number of skin sites.

In this study we evaluate the sample size dependence of the oleic-acid-induced enhancement values introduced in our earlier work (Yu *et al*, 2001). Based on the methodology described below, the optimum number of skin sites that capture the global variations in transdermal transport was determined for the hydrophobic and the hydrophilic model permeants examined.

MATERIALS AND METHODS

Sample preparation Human cadaver skin (National Disease Research Interchange, Philadelphia, PA) was prepared following previously described methods (Yu *et al*, 2001). Sulforhodamine B (SRB), the model hydrophilic probe, and rhodamine B hexyl ester (RBHE), the model hydrophobic probe (Molecular Probes, Eugene, OR), were prepared at 0.33 mg per ml for both the control and the model chemical enhancer vehicles (Yu *et al*, 2001).

High-speed, two-photon microscope and data analysis Four hundred consecutive skin sites in a 2 mm by 2 mm area of each skin

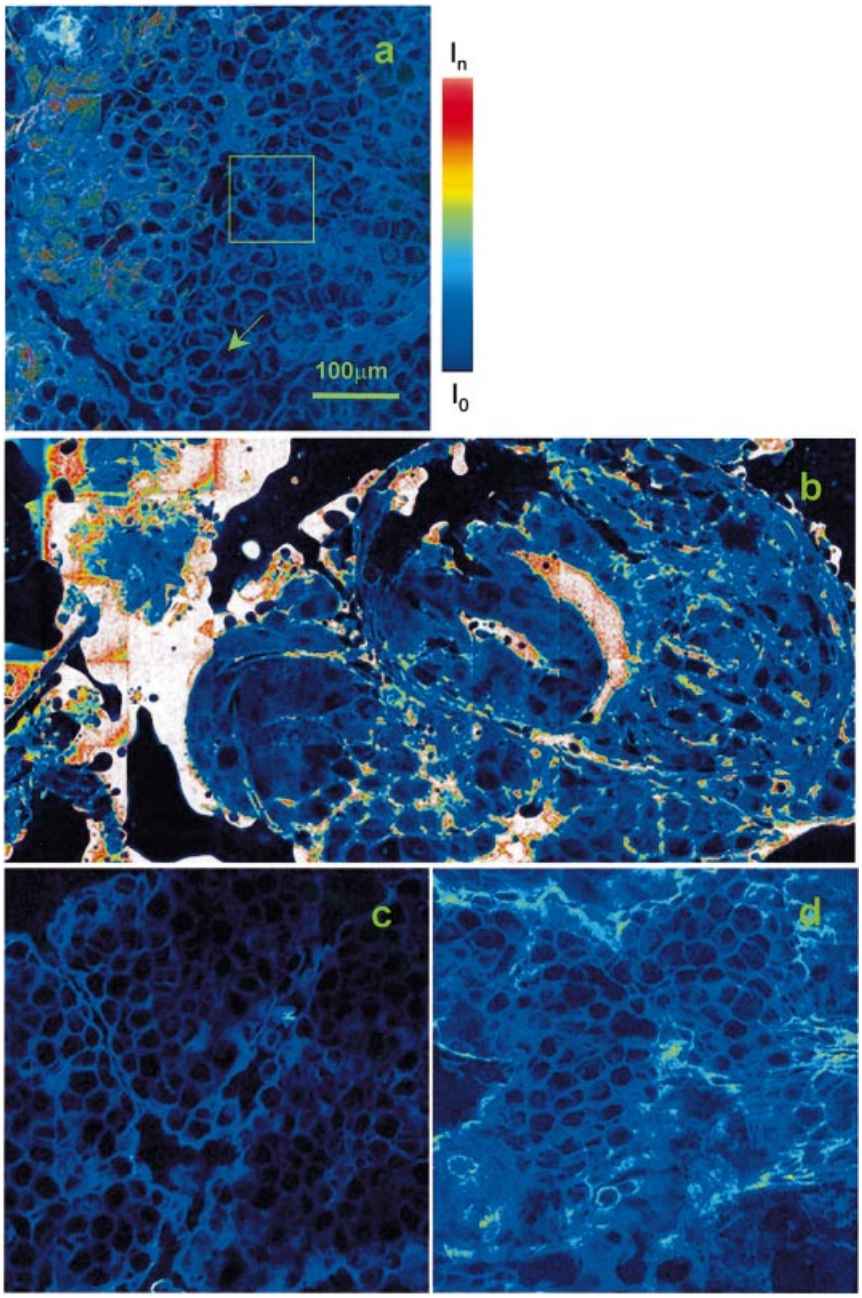

Figure 1. Visualization of fluorescent probe spatial distributions in the skin. Selected regions from the 4 mm^2 total skin area scanned are shown for (*a*)RBHE control, (*b*)RBHE oleic acid, (*c*)SRB control, and (*d*)SRB oleic acid cases of the probe distributions close to the skin surface. The *arrow* points to a circular dark region typical of stratum corneum corneocytes, whereas the intercorneocyte regions highlighted in blue represent the lipid multilamellae. The green box demarks the 100 μm by 100 μm area representing the field of view captured by the 40× objective for one individual skin site. The scale bar in (*a*) represents a length of 100 μm that is applicable to all the four cases examined. The color bar shows the pseudo-color scale, ranging from a low intensity of I_0 to a high intensity of I_n, utilized to represent the relative probe intensities. For (*a*), (*b*), (*c*), (*d*), $I_0 = 100$. To account for the increased range of intensities, $I_n = 3000$ for (*a*) and $I_n = 10{,}000$ for (*b*). $I_n = 5000$ for both (*c*) and (*d*). Regions of highest probe intensities are depicted in white.

sample were scanned from the skin surface to a depth of 21 μm (at 0.7 μm intervals) using the high-speed, two-photon microscope described in a separate study (Kim *et al*, 1999). The 400 different consecutive skin sites (each with an area of 100 μm by 100 μm) were computationally stitched together at a specified skin depth. The islands of dark regions, most apparent in **Fig 1(*b*)**, reflect locations of incomplete stratum corneum contact with the microscope slide coverslip due to the skin surface roughness, and have been omitted from the data quantification results presented below.

The quantification methodology that we introduced recently (Yu *et al*, 2001) was applied in this study to determine the enhancement values. In the previous study based on four to six skin sites (Yu *et al*, 2001), the relative change in the probe vehicle to skin partition coefficient, E_K, was defined as the ratio of the average probe intensities at the surface of the skin ($z = 0$) for the enhancer and the control samples. In the 400-skin-site study presented here, E_K is redefined as the ratio of the zero-order linear regression coefficients (the intercepts) of the linear region of the wide-area average intensity profile for the enhancer and the control cases. This linearly regressed value reflects the probe intensity at the surface of the skin where $z = 0$ μm, and yields a 95% confidence interval that reduces the error contributions to E_K.

Determination of representative skin sample sizes For each sample size (6, 12, 24, and 48 skin sites), 10 different sets of transport enhancement values for each probe were calculated based on 10 randomly selected sets of skin sites from the control and the enhancer skin samples. For each sample size, the relative variation V from the wide-area values calculated for each transport enhancement property were quantified utilizing the following equation (Johnson, 2000):

$$V = \frac{1}{\langle E \rangle}\left[\frac{\sum_i^N (E_i - \langle E \rangle)^2}{(N-1)}\right]^{1/2} \quad (1)$$

where N denotes the 10 different sets of skin sites associated with each sample size evaluated, E_i represents the transport property enhancement value obtained for data set i, and $<E>$ is the wide-area value of the transport property enhancement.

RESULTS AND DISCUSSION

Visualization of wide-area axial scans For each skin sample, a selected fraction of the total 4 mm^2 skin area evaluated is shown in

Fig 1. **Figures 1(*a–d*)** depict the spatial heterogeneity of probe distributions captured over a small portion of the total skin area imaged. The green box in **Fig 1**(***a***) represents the area encompassed by one microscope field of view. For each image in **Fig 1**, a comparison of the probe spatial distributions covered by one field of view with the corresponding skin fraction shown illustrates the need to examine multiple skin sites to fully capture the site to site variations in permeant transport.

For both RBHE and SRB, oleic-acid-induced increases in the probe partitioning into the stratum corneum are revealed by the increased intercellular probe intensities that are represented by the light blue regions in the color scale shown in **Fig 1**. In addition to the increased probe distribution throughout the intercorneocyte regions, **Fig 1**(***b***) illustrates an increase in the heterogeneity of the probe distribution, with regionalized areas of high probe concentration (regions in white).

In contrast to the similar probe intensity distributions observed in an overwhelming majority of the 400 skin sites scanned for the RBHE control (**Fig 1***a*), **Fig 1**(***c***) illustrates the nonuniform spatial distribution of the hydrophilic probe SRB typical of the 2 mm by 2 mm area scanned. The black to dark blue colors marking the intercellular regions observed in **Fig 1**(***c***) reflect the low skin permeabilities to hydrophilic permeants such SRB. Furthermore, the lighter blue regions in **Fig 1**(***c***) illustrate a localization of SRB transport that is consistent with the proposed existence of aqueous ''shunt'' transport pathways (Scheuplein, 1967; Sznitowska *et al*, 1998). In the presence of oleic acid, the overall increase in SRB skin penetration is accompanied by the appearance of distinct intercellular regions of higher probe concentrations that are highlighted in light blue (see **Fig 1***d*).

The wide-area axial scans presented in **Fig 1** unquestionably demonstrate the advantages of HTPM in efficiently increasing the sample area (100-fold) to provide a dramatically improved visualization of the range of variation in probe distributions over a clinically more relevant area of skin (2 mm by 2 mm). From these scans, the skin area represented by one field of view (100 μm by 100 μm) clearly does not validly capture the variability of the probe distributions over the 400 consecutive skin sites scanned.

Quantification of relative changes in transport properties As shown in **Fig 2**, the predominant effects of oleic acid action based on the 400-skin-site analysis for the hydrophilic (SRB) and the hydrophobic (RBHE) probes are the enhancements in the vehicle to skin partitioning (E_K = 4.77 ± 0.83 and 10.22 ± 0.55, respectively) and in the concentration gradient (E_g = 4.81 ± 1.86 and 9.93 ± 1.50, respectively). The physically pertinent E_l values of approximately unity obtained for both probes indicate that the strateum corneum remains the primary barrier to transdermal transport, and bring greater validity to relative changes in transport properties calculated for both probes based on the 100-fold increase in sample size.

Good agreement exists for the hydrophobic probe E_K, E_g, E_D, and E_l values between the 400-skin-site study (**Fig 2**, *gray bars*) and the previous four to six site study (**Fig 2**, *black bars*). The changes in the transport properties for the hydrophilic probe, however, exhibit a high degree of variability between these two very different skin sample sizes. This can be seen by comparing the white bars in **Fig 3**, which represent the 400-skin-site hydrophilic probe enhancement values, and the checkered bars in **Fig 3**, which represent the four to six skin site enhancement values. Moreover, the hydrophilic four to six skin site E_l value of 3.66 ± 1.67 predicts an increase in the skin barrier thickness, suggesting that, in the presence of oleic acid, the primary transport barrier extends beyond the stratum corneum layer. This E_l value deviates from unity and is inconsistent with the role of the stratum corneum as the primary barrier to transdermal transport.

Validity of limited site sampling in elucidating relative changes in transdermal transport properties To address the inconsistency found between the hydrophilic probe enhancement values based on four to six skin sites and the values obtained based on the 400-skin-site analysis, sample sizes reflecting a smaller number of skin sites (6, 12, 24, and 48 sites) were evaluated for both the hydrophilic and the hydrophobic probes to determine the feasibility of inferring chemical enhancer induced changes in global transport properties based on a limited sample size.

The relative insensitivity of the enhancement values to sample size for the hydrophobic probe is further substantiated by the mild

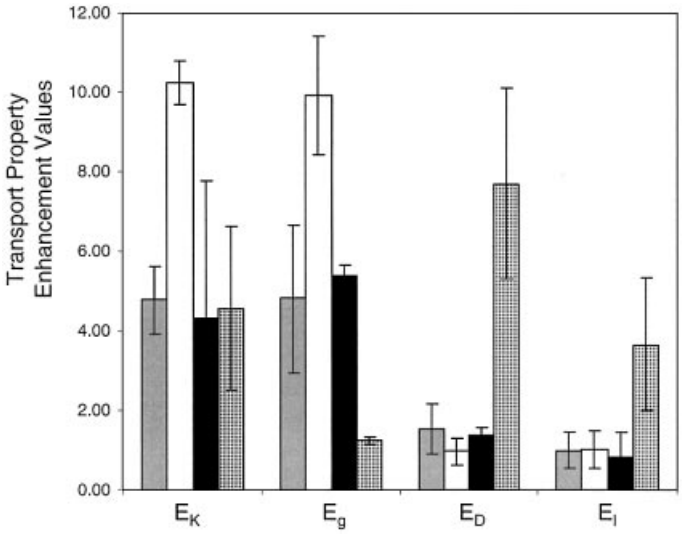

Figure 2. Relative changes in oleic-acid-induced transport. Key: 400 skin site RBHE (*gray bar*), 400 skin site SRB (*white bars*), RBHE limited sample size (*black bars*), SRB limited sample size (*checkered bars*). The wide-area values correspond to the transport enhancement values obtained in this study utilizing the data from the 400 skin sites scanned, whereas the limited sample size values refer to those reported recently by us (Yu *et al*, 2001) based on four to six skin sites. In the recent study based on four to six skin sites (Yu *et al*, 2001), E_K = 4.33 ± 3.45 and 4.56 ± 2.05, E_g = 5.37 ± 0.26 and 1.24 ± 0.09, E_l = 0.81 ± 0.64 and 3.66 ± 1.67, and E_D = 1.37 ± 0.20 and 7.70 ± 2.41 for the hydrophobic and the hydrophilic probes, respectively. The corresponding enhancement values obtained from the 400 skin sites scanned in this study are E_K = 4.77 ± 0.83 and 10.22 ± 0.55, E_g = 4.81 ± 1.86 and 9.93 ± 1.50, E_l = 0.99 ± 0.46 and 1.03 ± 0.47, and E_D = 1.53 ± 0.62 and 0.97 ± 0.33 for the hydrophobic and the hydrophilic probes, respectively. All the enhancement values are based on the previously reported E_P = 7.35 ± 1.00 and E_P = 9.59 ± 2.92 (Yu *et al*, 2001), for the hydrophobic and the hydrophilic probes, respectively. The error bars represent 1 SD from the mean.

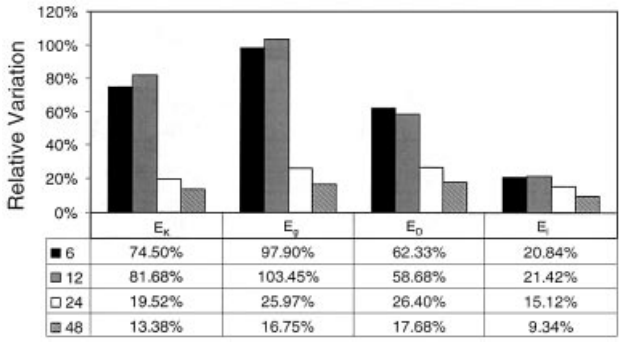

	E_K	E_g	E_D	E_l
6	74.50%	97.90%	62.33%	20.84%
12	81.68%	103.45%	58.68%	21.42%
24	19.52%	25.97%	26.40%	15.12%
48	13.38%	16.75%	17.68%	9.34%

Figure 3. Hydrophilic probe transport property enhancement relative variation. Key: 6 skin sites (*black bars*), 12 skin sites (*gray bars*), 24 skin sites (*white bars*), and 48 skin sites (*striped bars*). The strong dependence of the relative variation (see Eqn 1), reported in percentage form along the *y* axis, is shown as a function of the sample size on the *x* axis for each transport enhancement value. The data table below the chart lists the values of the relative variations calculated at each sample size for each different enhancement value.

decreases in the relative variation V calculated from Eqn 1 with increases in sample size. Fractional deviations of approximately 36%, 27%, 40%, and 33% were obtained for the hydrophobic E_K, E_g, E_D, and E_l values using the six-skin-site sample size. Increasing the sample size to 48 skin sites decreases the relative variance values to approximately 17%, 21%, 26%, and 15%, respectively. In optimizing the sample size, increasing the sample size beyond six skin sites does not provide substantial increases in the accuracy. Considering the variations in the human skin permeabilities described in the literature, with intersample variations in drug permeability as large as 40% (Southwell *et al*, 1984) and intrasample drug permeability variations of 20%–30% (Noonan and Gonzalez, 1990), the relative variances of enhancement values resulting from a six-skin-site sample size fall within the range of variation expected due to the inherent heterogeneity of the skin morphology.

For the hydrophilic probe, however, **Fig 3** shows the strong dependence of V on the four different sample sizes evaluated. Compared to the six-skin-site V values for E_K, E_g, E_D, and E_l of 75%, 98%, 62%, and 21%, respectively, significantly decreased values of approximately 13%, 17%, 18%, and 9%, respectively, were obtained using the 48-skin-site sample size. The optimum sample size for the hydrophilic probe is 24 skin sites, at which the maximum decrease in the relative variance is observed with the least number of increases in the skin sites. At the 24-skin-site sample size, the relative variance values of approximately 15%–26% all fall within the criteria cited above that describe the expected variability of human skin.

The variations in the probe spatial distributions observed over the 400 consecutive skin sites imaged suggest that, for future applications of other microscopy visualization techniques, the validity of the global changes in skin barrier function deduced from the evaluation of a limited skin sample size warrants additional scrutiny.

This research was supported by a National Institutes of Health grant GM44884. The authors would like to thank Professor Michael Holick for providing insightful guidance regarding the HTPM studies. Also, we would like to thank Professor Sidney Yip for helpful discussions on the analysis of sample size effects.

REFERENCES

Huzaira M, Rius F, Rajadhyaksha M, Anderson RR, González S: Topographic variations in normal skin, as viewed by *in vivo* reflectance confocal microscopy. *J Invest Dermatol* 116:846–852, 2001

Johnson RA: *Miller and Freund's Probability and Statistics for Engineers*. Upper Saddle River, NJ: Prentice Hall, 2000

Kim KH, Buehler C, So PTC: High-speed, two-photon scanning microscope. *Appl Optics* 38:6004–6009, 1999

Masters BR, So PTC, Gratton E: Multiphoton excitation fluorescence microscopy and spectroscopy of *in vivo* human skin. *Biophys J* 72:2405–2412, 1997

Noonan PK, Gonzalez MA: Pharmacokinetics and the variability of percutaneous absorption. *J Toxicol Cut Ocular Toxicol* 8:511–516, 1990

Scheuplein RJ: Mechanism of percutaneous absorption. *J Invest Dermatol* 48:79–88, 1967

Southwell D, Barry BW, Woodford R: Variations in permeability of human skin within and between specimens. *Int J Pharm* 57:299–309, 1984

Sznitowska M, Janicki S, Williams AC: Intracellular or intercellular localization of the polar pathway of penetration across stratum corneum. *J Pharm Sci* 87:1109–1114, 1998

Yu B, Dong C-Y, So PTC, Blankschtein D, Langer R: *In vitro* visualization and quantification of oleic acid induced changes in transdermal transport using two-photon fluorescence microscopy. *J Invest Dermatol* 117:16–25, 2001